Title

Chemerin regulates formation and function of brown adipose tissue: Ablation results in increased insulin resistance with high fat challenge and aging

Journal

The FASEB Journal, 35(7)

ISSN

0892-6638

Authors

Zhang, Yiqiang
Shen, Wen-Jun
Qiu, Shuo
et al.

Publication Date

2021-07-01

DOI

10.1096/fj.202100156r

Peer reviewed

HHS Public Access

Author manuscript

FASEB J. Author manuscript; available in PMC 2022 March 28.

Published in final edited form as:

FASEB J. 2021 July ; 35(7): e21687. doi:10.1096/fj.202100156R.

Chemerin regulates formation and function of brown adipose tissue: Ablation results in increased insulin resistance with high fat challenge and aging

Yiqiang Zhang[1,2,3], **Wen-Jun Shen**[1,2], **Shuo Qiu**[1,2], **Pinglin Yang**[1,2,4], **Garrett Dempsey**[5], **Lei Zhao**[2,6], **Qin Zhou**[2,6], **Xiao Hao**[1,2,7], **Dachuan Dong**[1,2], **Andreas Stahl**[5], **Fredric B. Kraemer**[1,2], **Lawrence L. Leung**[2,6], **John Morser**[2,6]

[1]Division of Endocrinology, Department of Medicine, Stanford University School of Medicine, Stanford, CA, USA

[2]Veterans Affairs Palo Alto Health Care System, Palo Alto, CA, USA

[3]Department of Biochemistry, Changzhi Medical College, Changzhi, China

[4]Department of Orthopedics, Second Affiliated Hospital of Xi'an Jiaotong University, Xi'an, China

[5]Department of Nutritional Sciences and Toxicology, University of California at Berkeley, Berkeley, CA, USA

[6]Division of Hematology, Department of Medicine, Stanford University School of Medicine, Stanford, CA, USA

[7]Department of Endocrinology, The First Affiliated Hospital of the Medical College of Zhengzhou University, Zhengzhou, China

Abstract

Apart from its role in inflammation and immunity, chemerin is also involved in white adipocyte biology. To study the role of chemerin in adipocyte metabolism, we examined the function of chemerin in brown adipose tissue. Brown and white adipocyte precursors were differentiated into adipocytes in the presence of Chemerin siRNA. Chemerin-deficient (*Chem*$^{-/-}$) mice were compared to wild-type mice when fed a high-fat diet. Chemerin is expressed during brown adipocyte differentiation and knock down of chemerin mRNA results in decreased brown adipocyte differentiation with reduced fatty acid uptake in brown adipocytes. *Chem*$^{-/-}$ mice are leaner than wild-type mice but gain more weight when challenged with high-fat diet feeding, resulting in a larger increase in fat deposition. *Chem*$^{-/-}$ mice develop insulin resistance when on a

Correspondence: John Morser and Wen-Jun Shen, Veterans Affairs Palo Alto Health Care System, Building 101-4A131, 3801 Miranda Avenue, Palo Alto, CA 94304, USA. jmorser@stanford.edu (J. M.) and wen-jun@stanford.edu (W. S.).

AUTHOR CONTRIBUTIONS

F.B. Kraemer, L.L. Leung, J. Morser, and W.-J. Shen designed the experiments, Y. Zhang, W.-J. Shen, S. Qiu, X. Hao, P. Yang, and D. Dong performed the research, L. Zhao ran the chemerin ELISAs, G. Dempsey, W.-J. Shen and Q. Zhou performed the animal experiments, W.-J. Shen, A. Stahl, F.B. Kraemer, L.L. Leung, and J. Morser analyzed the data, W.-J. Shen and J. Morser wrote the first draft and all authors reviewed the manuscript before submission.

CONFLICTS OF INTEREST

The authors declare no conflicts of interest.

SUPPORTING INFORMATION

Additional Supporting Information may be found online in the Supporting Information section.

high-fat diet or due to age. Brown adipose depots in *Chem*$^{-/-}$ mice weigh more than in wild-type mice, but with decreased mitochondrial content and function. Compared to wild-type mice, male *Chem*$^{-/-}$ mice have decreased oxygen consumption, CO_2 production, energy expenditure, and a lower respiratory exchange ratio. Additionally, body temperature of *Chem*$^{-/-}$ mice is lower than that of wild-type mice. These results revealed that chemerin is expressed during brown adipocyte differentiation and has a pivotal role in energy metabolism through brown adipose tissue thermogenesis.

Keywords

adipocytes; adipokines; chemerin; energy balance

1 | INTRODUCTION

With the discovery of leptin and adiponectin, adipose tissue has been recognized as an important endocrine and immune organ involved in the regulation of metabolic homeostasis of the whole body. Mammalian adipose tissue consists of white and brown adipocytes. Typically white adipocytes, located in WAT, have a single large triacylglyceride lipid droplet and few mitochondria and are more specialized for energy storage, in addition to being a source of adipokines. In contrast, brown adipocytes have many small lipid droplets and a much higher concentration of mitochondria with uniquely high expression of uncoupling protein 1 (UCP1). UCP1 is localized on the inner mitochondrial membrane and functions to uncouple oxidative phosphorylation from ATP production and release energy as heat. Therefore, BAT is specialized for energy expenditure and nonshivering thermogenesis. Although BAT was previously viewed as only active in babies, advances in imaging techniques and recent morphological studies reveal the presence and activity of BAT in adult humans. At normal ambient temperature, white and brown adipocytes are present in several subcutaneous and visceral depots in mice.[1–5] In obese animals and humans, however, most of the typical brown adipocytes convert into a “white-like” phenotype[6,7] and are therefore barely detectable.

A hallmark of metabolic syndrome is insulin resistance. Adipokines, bioactive peptides and proteins secreted from adipose tissues are markedly dysregulated in obesity, type 2 diabetes and metabolic syndrome,[8] with these metabolic abnormalities being linked to a chronic inflammatory state.[9] Chemerin (aka retinoic acid receptor responder protein 2; RARRES2) is a chemoattractant that is positioned at the interface between thrombosis, inflammation, and immunity and plays an important role in adipocyte biology and metabolism.[10] It binds to and signals through chemokine-like receptor 1 (CMKLR1, aka ChemR23) and GPR-1, both G-protein coupled receptors (GPCRs),[11] and binds to, but does not signal through, chemokine (C-C motif) receptor-like 2 (CCRL2).[12,13] Chemerin, CMKLR1, and GPR1 are highly expressed in mouse and human adipocytes.[14] Cultured 3T3-L1 adipocytes secrete chemerin, leading to chemotaxis of CMKLR1-expressing cells. In addition, by recruiting dendritic cells (DCs), chemerin may be important in the initiation and propagation of inflammation and the development of insulin resistance and the metabolic syndrome.[15]

Chemerin is secreted from the liver and adipose tissue as well as by other cells as an inactive precursor that is then activated by various proteases associated with the coagulation cascade, fibrinolysis, and inflammation and then subsequently proteolytically inactivated.[16–20] The levels and prevalence of the different active and inactive forms of chemerin vary with obesity and insulin resistance.[20–22]

White adipocyte differentiation in vitro is dependent on production and activation of chemerin.[14,23] When cells are treated with siRNA to knockdown either chemerin or CMKLR 1 expression before initiating differentiation, differentiation of 3T3-L1 cells into adipocytes is impaired and the expression of genes involved in glucose and lipid homeostasis such as GLUT4 and adiponectin is reduced. After 4 days of differentiation, however, knockdown of chemerin or CMKLR1 expression does not affect adipocyte morphology.[14] Chemerin treatment of 3T3-L1 adipocytes increases glucose uptake as well as the insulin signaling molecule, IRS-1.[24]

We had previously documented that chemerin protein was detected in brown adipose tissue,[20] but its expression and function in brown adipose tissue has not been explored. In this paper, we report the role of chemerin during brown adipocyte differentiation and subsequent metabolic changes in chemerin-deficient (*Chem*$^{-/-}$, *Rarres2*$^{-/-}$) mice with high-fat diet and cold challenges.

2 | METHODS AND MATERIALS

2.1 | Chemicals and reagents

All chemicals were obtained from Sigma-Aldrich (St. Louis, MO) unless otherwise specified. Cholesterol LiquiColor Test (Enzymatic) was from Stanbio (Boerne, TX, USA); serum non-esterified fatty acid kit from Fujifilm Wako Diagnostic USA (Mountain View, CA); serum glycerol kit from Sigma-Aldrich (St. Louis, MO); bicinchoninic acid assay protein kit from Pierce Biotechnology, Inc (Rockford, IL, USA); organic solvents from J. T. Baker (Phillipsburg, NJ, USA); TRIzol reagent and SuperScript II from Invitrogen (Carlsbad, CA, USA); RNeasy kit from QIAGEN (Valencia, CA, USA); SyBr green Taqman PCR kit from Applied Biosystems (Foster City, CA, USA); M-040274-01-0005 siGENOME siRNA for mouse Rarres2 (71660) from Dharmacon, Inc, (Chicago, IL, USA); mouse chemerin monoclonal antibody (R and D Systems Cat# MAB2325, RRID: AB_2238042), biotinylated anti mouse chemerin polyclonal goat IgG (R and D Systems Cat# BAM2325, RRID: AB_1964540), and recombinant mouse chemerin protein from R&D systems, Inc (Minneapolis, MN, USA); Bio-Rad protein assay dye reagent concentrate from Bio-Rad Laboratories, Inc (Hercules, CA, USA).

2.2 | Animals

Animal studies were performed at the Veterans Administration Palo Alto Health Care System (VAPAHCS), Palo Alto, CA, or University of California, Berkeley, in accordance with National Institutes of Health guidelines. All procedures were approved by the institutional animal care and use committee of either VAPAHCS or University of California, Berkeley. Mice were housed in the animal facility with normal chow diet (TK 2918, Envigo,

Huntingdon, UK) and water available ad libitum in 12 hours/12 hours dark-light cycle and temperature (22–25°C) controlled environment. *Chem*$^{-/-}$ mice were obtained from Deltagen (San Mateo, CA, USA) on a C57Bl6/N background and were backcrossed more than 10 times onto a C57Bl6/J background. wild-type C57Bl6/J (WT) controls were from Jackson Laboratory (Sacramento, CA). Male and female matching WT and *Chem*$^{-/-}$ mice (6 weeks old, n = 6–8) were switched to either a high-fat (HF) Western diet (D12492 for diet-induced obesity, 60% fat, 7% sucrose, Research diets Inc, New Brunswick, NJ) or a low-fat (LF) control diet (D12450J, 10% fat, 7% sucrose, Research Diets Inc) ad libitum with continuously available water and maintained on this diet for 8 weeks. Intraperitoneal glucose tolerance test (ipGTT) and intraperitoneal insulin tolerance test (ipITT) were performed on the animals at 14 weeks of age; body composition was analyzed before switching to the different diets and after being on those diets for 8 weeks. At the end of diet treatment, animals were sacrificed, blood collected by cardiac puncture and tissues weighed, collected and frozen for further analysis. ipGTT and ipITT were also performed on WT and *Chem*$^{-/-}$ mice that were on normal chow diet for 6 months (25–28 weeks).

2.3 | Intraperitoneal glucose tolerance test (ipGTT)

Prior to glucose challenge, the mice were fasted overnight (~14–16 h) by transferring them to clean cages with no food available but free access to drinking water. Glucose (0.2 g/mL in saline) was injected ip to achieve a glucose dose of 1 g/kg. Blood glucose levels were measured using a Bayer Contour Glucometer and test strips immediately prior to (0 min) and 15, 30, 60 and 120 minutes post glucose injection. The area of the blood glucose response profile curve for each animal was calculated by the trapezoid method,[5] using as reference each individual's baseline blood glucose. The trapezoidal areas between the 0, 15, 30, 60 and 120 minutes time points were summed to obtain the area under the curve (AUC).

2.4 | Intraperitoneal insulin tolerance test (ipITT)

For ipITT, animals were fasted for 6 hours. Insulin (Humulin-R-100, Eli Lilly) was injected ip at a dose of 0.75 U/kg and blood glucose levels were measured immediately prior to (0 min) and 15, 30, 45, and 60 minutes post insulin injection. The resultant changes in glucose levels for each mouse were used to calculate AUC for response to insulin, as described above.

2.5 | Body composition analysis

The body composition of the mice was analyzed by Dual Energy X-Ray Absorptiometry (DXA). Animals anesthetized with isoflurane (1.5%) were placed in the viewfinder of the UltraFocus^{DXA} Scanner (Faxitron Bioptics LLC, Tucson, AZ, USA), and scanned following the manufacturer's guideline. Body composition including total weight, fat content (fat weight and fat %), lean weight and soft weight were calculated.

2.6 | Metabolic analysis using Comprehensive Laboratory Animal Monitoring System (CLAMS)

For metabolic analysis using metabolic cages, four-month old age-matched male WT and *Chem*$^{-/-}$ mice (n = 4/group) were studied using a CLAMS at University of California,

Berkeley. Animals were housed at 23°C with 12 hours light and dark cycle. Animals were acclimatized to single housing in a cage overnight, then transitioned to 12°C for 4 hours before reducing the temperature to 4°C for 6 hours before returning back to 23°C. Measurements of oxygen consumption, CO_2 production, movement, energy expenditure, and respiratory exchange ratio were carried out over a period of 46 hours. Data were analyzed by calculating the AUC for each temperature duration and presented as means ± SEM.

2.7 | Histological analysis of tissues

Liver, white adipose tissue (WAT), and brown adipose tissue (BAT) samples were collected at the time of sacrifice and fixed with 4% paraformaldehyde before paraffin embedding, sectioning and staining with H&E by Histo-tech laboratory (Hayward, CA, USA). Fat cell area was quantitated with ImageJ.

2.8 | Stimulated lipolysis

After 8 weeks on high-fat diet, lipolysis in mice was stimulated with an ip injection of 10mg/kg isoproterenol. Serum samples were collected before and 15 minutes after stimulation and serum FFAs and glycerol were analyzed using kits from Fujifilm Wako diagnostic USA and Sigma-Aldrich, respectively.

2.9 | Quantitative real time PCR (qPCR)

WAT and BAT samples were homogenized in 1 mL of TRIzol reagent using a power homogenizer (Ultra-Turrax T10 basic, IKA-Works, Wilmington, DE, USA) to extract total RNA. After ethanol precipitation, total RNA was dissolved in 20–50 μL ribonuclease-free water, then converted to cDNA with SuperScrip IV Reverse Transcriptase (ThermoFisher Scientific) for real-time PCR analysis on an ABI Prism 8500 System (Applied Biosystems, Foster City, CA, USA) using SYBR green master mix reagent and the primer pairs listed in Table 1. Gene expression was calculated by the delta-delta CT method using the control housekeeping gene 36B4, a ribosomal protein, for normalization.

2.10 | Cell lines and cell culture

Mouse embryonic stem cells, OP9 (CRL-2749), were obtained from American Type Culture Collection (ATCC, Manassas, Virginia) and grown in Eagle's Minimum Essential Medium (MEM) (Alpha Modification) with deoxyribonucleosides, ribonucleosides, L-glutamine, 20% fetal bovine serum, penicillin (100 U/mL), and streptomycin (100 μg/mL) (Invitrogen/Life Technologies Corporation, Long Island, NY, USA). The brown pre-adipocyte cell line, SBAT, was a kind gift from Dr Shingo Kajimura (Harvard University) and maintained in Dulbecco's modified Eagle's low glucose medium supplemented with 10% fetal bovine serum (DMEM-FBS), glutamine, pyruvate, penicillin (100 U/mL), and streptomycin (100 μg/mL).

OP9 and SBAT cells were both grown to confluency and then treated with a differentiation cocktail to initiate differentiation. For OP9 cells, cells were differentiated first with complete growth medium supplemented with 1 μM dexamethasone and 0.5 mM 3-isobutyl-1-methylxanthine. After 2 days, the medium was replaced with complete growth media with 1 μg/mL insulin to stimulate lipid accumulation. Aliquots were collected on days 0, 3, 5, and 7

to determine chemerin levels by ELISA. For SBAT differentiation, cells in complete growth media were treated with 5 μg/mL insulin, 1 nM triiodothyronine, 0.125 mM indomethacin, 2 μg/mL dexamethasone, and 0.5 mM 3-isobutyl-1-methylxanthine. After 2 days, the medium was replaced with complete growth media with 5 μg/mL insulin and 1 nM triiodothyronine to stimulate lipid accumulation. Aliquots were collected on days 0, 3, 5, and 7 to determine chemerin levels by ELISA.[20] Cell cultures were stained with mito-tracker (red) and bodipy-FA (green) before quantitating the area of lipid droplets with ImageJ.

2.11 | Fatty acid uptake assay

OP9 or SBAT cells were seeded into a black-wall/clear-bottom 96-well plate (Costar), transfected with Chemerin Pre-designed Silencer Select siRNA or scrambled siRNA following a reverse transfection protocol and then cultured for 5 days for OP9 cells or 7 days for SBAT cells, respectively, according to the differentiation protocol described above. After differentiation, a fatty acid uptake assay was performed.[25] Briefly, the medium was removed from the wells and replaced with 90 μL/well serum free medium and 10 μL/well HBSS (1x) containing 0.2% fatty acid-free BSA. The assay plate was then incubated for one hour at 37°C in 5% CO_2. A zero time read was performed before 100 μL of Bodipy-dodecanoic acid in HBSS (1x) containing 0.2% BSA, was added to each well and immediately read in a fluorescence microplate reader with a reading every 30 seconds for 30 minutes at 485nm using bottom-read mode.

2.12 | Statistical analysis

Statistical analysis was performed using Prism (Prism 8.0, GraphPad, San Diego, CA). All of the data are expressed as the mean ± SEM. Data were analyzed by Student's *t* test with $P < .05$ considered significant. When more than 2 groups were compared, one-way ANOVA analysis was performed with Bonferroni's multiple comparison test post hoc with $P < .05$ considered significant.

3 | RESULTS

3.1 | Chemerin is expressed during brown adipocytes differentiation

Earlier, chemerin had been detected in brown adipose tissue[20] with the level of chemerin in brown adipose correlating with weight and % body fat, in contrast to chemerin levels in epididymal fat, which were inversely correlated with weight and % body fat. To explore the functional significance of chemerin in brown adipocytes, brown adipocyte precursor cells (SBAT) were grown to confluency and induced to differentiate for 7 days. Brown adipocytes accumulated multiple small lipid droplets along with high numbers of mitochondria (Figure 1A). As a control, white adipocytes, which were differentiated for 5 days from the OP-9 precursor cell line, displayed larger lipid droplet(s) with fewer mitochondria. When the precursor cells were transfected with chemerin siRNA, there was a ~40% decrease in chemerin mRNA (Figure S1), differentiation was decreased and there was less lipid droplet accumulation in both brown and white adipocytes compared to cells transfected with control siRNA (Figure 1C,E). Changes in levels of mRNA markers (C/EBPβ, PRDM-16 and PREF-1) for brown or white adipocyte differentiation, determined by PCR, were consistent with brown or white adipocyte differentiation (Figure S1). This suggests that chemerin is

involved in the differentiation of both types of adipose cells. Chemerin mRNA expression increased by ~25 fold at day 7 after initiation of differentiation in brown adipocytes (Figure 1B) and mRNA encoding all 3 chemerin receptors could be detected in differentiated brown adipocytes. The time course of the increase in chemerin and its receptors was similar for brown and white adipocyte differentiation. Quantitation of chemerin in the culture medium by ELISA showed increased chemerin in the media at day 7 in both types of adipocyte (Figure 1D,F).

Fatty acid uptake was analyzed after the adipocytes were fully differentiated. BAT adipocytes treated with chemerin siRNA had decreased fatty acid uptake while chemerin siRNA treatment of WAT adipocytes increased fatty acid uptake (Figure 2A).

There was increased expression of genes involved in fatty acid esterification in BAT adipocytes with knockdown of chemerin mRNA when examined by qPCR (Figure 2B). With ~40% knockdown of chemerin mRNA, the differentiated WAT adipocytes showed a trend toward increased expression of genes involved in fatty acid esterification. There was, however, a significant increase in FATP1 and CD36 expression in WAT adipocytes with knockdown of chemerin mRNA. These data show that after chemerin siRNA treatment of brown and white adipocytes, differentiation is decreased with fewer cells undergoing differentiation. Chemerin mRNA knockdown in differentiated brown adipocytes led to increased fatty acid uptake in contrast to white adipocytes where fatty acid uptake decreased.

3.2 | *Chem*$^{-/-}$ mice gain more weight than WT mice on a HF diet

To study the physiological role of chemerin, *Chem*$^{-/-}$ mice and wild-type mice were fed either LF or HF diets for eight weeks and weight gain, food intake and body temperature were monitored. Male *Chem*$^{-/-}$ mice, but not female, gained less weight during the eight weeks diet period on low-fat diet than sex matched WT mice (Figure 3A). On high-fat diet, female *Chem*$^{-/-}$ mice gained more weight than WT mice (Figure 3B). The body temperature was monitored and so was the food intake. At 14 weeks old, the core body temperature for male WT mice on HF diet was higher than that of either male or female *Chem*$^{-/-}$ mice (Figure 3C). This was not due to differences in food intake as there was no change in food intake (Figure 3D).

3.3 | *Chem*$^{-/-}$ mice show a larger increase in fat deposition with HF feeding than WT mice

When the body composition was analyzed with DXA, we found that male *Chem*$^{-/-}$ mice had lower fat weight and percentage fat on the LF diet than WT mice (Figure 4A,B, both $P <$ .05). In contrast, the *Chem*$^{-/-}$ mice had a greater increase in fat deposition after eight weeks of HF diet measured as either fat weight or percentage fat in both genders than WT mice (Figure 4A,B; both $P < .01$). There was decreased lean weight (Figure 4C) in both male and female *Chem*$^{-/-}$ mice after high-fat feeding ($P < .001$). Soft tissue weight, which includes both the lean weight and the fat weight, was decreased in male *chem*$^{-/-}$ mice compared to WT mice on LF diet (Figure 4D). With HF feeding, however, there was an increase of soft tissue weight in *Chem*$^{-/-}$ mice, especially in females compared to WT mice ($P < .05$). Bone mineral content was lower in *Chem*$^{-/-}$ mice than WT mice with LF feeding (Figure 4E; $P <$

.05). The bone mineral density was reduced in the *Chem*$^{-/-}$ mice compared to WT mice in both male and female mice on either diet (Figure 4F).

3.4 | *Chem*$^{-/-}$ mice develop insulin resistance with HF feeding or aging

To assess metabolic changes in the *Chem*$^{-/-}$ mice, ipGTTs and ipITTs were performed on 15-week old mice fed on either LF or HF diets in comparison to WT mice. *Chem*$^{-/-}$ mice have similar glucose tolerance as WT mice irrespective of the diet (Figure 5A,C). *Chem*$^{-/-}$ mice on low-fat diet had a similar response to insulin as WT mice (Figure 5B) but had increased insulin resistance compared to WT mice in both genders on high-fat diet (Figure 5D, for male $P < .05$, for female $P < .01$).

As aging increases metabolic abnormalities,[26,27] we tested ipGTT and ipITT challenges in six-month-old *Chem*$^{-/-}$ and WT mice fed normal chow. Similar to the results of younger mice on HF diet, male *Chem*$^{-/-}$ mice were more insulin resistant than six-month-old WT mice on the normal chow diet but there was no difference in glucose tolerance in either gender of WT or *Chem*$^{-/-}$ mice (Figure 5E,F, $P < .05$).

3.5 | Male *Chem*$^{-/-}$ mice have decreased oxygen consumption, CO_2 production, decreased energy expenditure, and lower respiratory exchange ratio compared to WT mice

Brown adipocytes are highly specialized for non-shivering thermogenesis with a large number of mitochondria per cell with increased UCP1 expression.[28] To analyze the effects of chemerin deficiency on energy consumption and response to cold challenges, age-matched male WT and *Chem*$^{-/-}$ mice fed normal chow were placed in metabolic cages and oxygen consumption, CO_2 production, energy expenditure, respiratory exchange ratio were measured. There was decreased oxygen consumption by *Chem*$^{-/-}$ mice compared to WT mice at 23°C (Figure 6A–C, $P < .05$), with a trend to decreased oxygen consumption at 12°C and 4°C. Similarly, CO_2 production was lower in *Chem*$^{-/-}$ mice than WT mice at 23°C (Figure 6D–F, $P < .05$), while there was a trend to decreased CO_2 production in *Chem*$^{-/-}$ mice at 12°C and 4°C. Total energy expenditure was also significantly decreased in *Chem*$^{-/-}$ mice compared to WT mice at 23°C (Figure 6G–I, $P < .05$), with a trend to reduced energy expenditure in *Chem*$^{-/-}$ mice at both 12°C and 4°C. A significant decrease in the respiratory exchange ratio was observed in the *Chem*$^{-/-}$ mice at both 4°C and 23°C, but not at 12°C (Figure 6J–L, $P < .01$ and $P < .001$, respectively), indicating a dysfunction in fuel utilization in mice with chemerin deficiency in which larger amounts of lipid are used to maintain their energy balance.

3.6 | Male *Chem*$^{-/-}$ mice have decreased FFA release in stimulated lipolysis

Stored energy is mobilized through hydrolysis of triglycerides and release of glycerol and fatty acids for utilization in metabolic pathways. To investigate this process in *Chem*$^{-/-}$ compared to WT mice on a HF diet, lipolysis was stimulated by administration of isoproterenol. Serum glycerol increased above the basal level in both WT and *Chem*$^{-/-}$ mice of both genders (Figure 7A), but FFA levels were two-fold higher in WT than *Chem*$^{-/-}$ male mice (Figure 7B; $P < .05$). When triglycerides are hydrolyzed, three FA molecules will be generated for each glycerol, but in *Chem*$^{-/-}$ mice the ratio was only ~1.3:1, in contrast to

that for the WT male mice[29] where the expected stoichiometry of ~3:1 was observed (Figure 7C, $P < .05$).

3.7 | *Chem*$^{-/-}$ mice have increased BAT and WAT

In order to investigate further the differences in weight gain between WT and *Chem*$^{-/-}$ mice after high-fat feeding, the liver, and various adipose tissue depots were weighed after sacrificing the animals at week 16. The liver weight was unaltered in *Chem*$^{-/-}$ mice whether on LF or HF diet (Figure 8A), but both visceral and subcutaneous white adipose tissue in various depots was increased in both male and female *Chem*$^{-/-}$ mice after HF feeding compared to WT mice, as was total white adipose tissue (Figure 8B–D). BAT was also increased in both male and female mice (Figure 8E).

3.8 | *Chem*$^{-/-}$ mice have increased size of brown and white adipocytes

As both WAT and BAT weights were increased in *Chem*$^{-/-}$ mice, we investigated if the structure of those tissues had been changed. An increased adipocyte size was observed in BAT from female *Chem*$^{-/-}$ mice on a LF diet compared to WT, which was more apparent when the female *Chem*$^{-/-}$ mice were on a HF diet (Figure 9A,B). Quantification of the area of white adipocytes in mice measured using Image J confirms the increase in white adipocyte size in female *Chem*$^{-/-}$ mice compared with control mice on both diets while male *Chem*$^{-/-}$ mice only displayed this phenotype on HF diet (Figure 9C–F). For both male and female *Chem*$^{-/-}$ mice, there was an increase in brown adipocyte size when animals were fed on either diet in comparison to WT mice with brown adipocyte size being larger when the mice were on a HF diet. As a control tissue that had similar weights in WT and *Chem*$^{-/-}$ mice, histological analysis of the liver showed no significant changes for mice on either LF or HF diets.

3.9 | Decreased expression of genes for mitochondrial function in BAT of *Chem*$^{-/-}$ mice

As BAT is characterized by high levels of mitochondria and increase of BAT weight and adipocyte size, we assessed changes in BAT in HF fed *Chem*$^{-/-}$ mice compared to WT mice by qPCR analysis of mitochondrial gene expression. Expression levels of the housekeeping proteins, mitochondrial cyclophilin D, and mitochondrial gatekeeper protein, VDAC1, were unchanged (Figure 10A). Male *Chem*$^{-/-}$ mice had decreased expression of genes involved in mitochondrial respiratory chain functional complexes such as mt-Cox1, mt-ND2, and mt-CytB ($P < .05$), while mt-Cox1 and mt-ND2 were also decreased in female *Chem*$^{-/-}$ mice compared to WT ($P < .05$) (Figure 10B). Expression of genes involved in the thermogenic functions of BAT, PRDM16, CPT1, and DIO2, was decreased in male *Chem*$^{-/-}$ mice ($P < .05$), while female *Chem*$^{-/-}$ mice had decreased expression of PRDM16 in their BAT (Figure 10C). Similar to what we had observed in adipocytes with knockdown of chemerin, BAT in *Chem*$^{-/-}$ mice show increased expression of genes involved in lipid accumulation, FATP-1 in male mice, and DGAT-2 in female mice (Figure 10D).

4 | DISCUSSION

Despite the distinct functions of BAT and WAT, brown and white adipocytes share a similar transcriptional cascade for adipocyte differentiation with different factors for cell

fate determination.[30] Chemerin plays a key role in white adipocyte differentiation[14] but it is unknown if it regulates brown adipocyte differentiation. We show here that both chemerin mRNA expression and levels of secreted chemerin increased significantly during differentiation of brown adipocytes. Reduction of chemerin expression with siRNA[2] resulted in fewer cells undergoing differentiation along with decreased lipid accumulation in differentiated brown adipocytes and decreased fatty acid uptake in the differentiated brown adipocytes. There was a slight increase in the expression of genes involved in fatty acid esterification such as DGAT1.

In comparison, reduction of chemerin expression in white adipocyte precursors also resulted in fewer cells differentiating into white adipocytes similarly to brown adipocytes, but there was increased fatty acid uptake together with increased expression of genes involved in fatty acid uptake such as FATP1 and CD36. Chemerin increases glucose uptake in WAT,[14,24,31–34] and we observed decreased glucose uptake upon chemerin knock down (data not shown). As both glucose and fatty acids can be used as an energy source for adipocytes, increased fatty acid uptake in the cells with chemerin knockdown could be a compensatory mechanism to maintain a steady energy source when glucose uptake is attenuated.

This effect of chemerin on lipid loading was also seen in *Chem*$^{-/-}$ mice when fed a HF diet. On a LF diet, male *Chem*$^{-/-}$ mice weigh less and have lower % body fat than WT mice, but when animals were fed a 60% HF diet, *Chem*$^{-/-}$ mice have a greater increase in adiposity when measured by DXA body composition analysis than WT mice. There were larger adipose depots comprising bigger adipocytes after eight weeks of HF feeding, and increased WAT adipocyte size by histological analysis in *Chem*$^{-/-}$ mice compared to WT mice.

There was a greater increase in the size of BAT adipocytes in *Chem*$^{-/-}$ mice than WT mice after HF diet feeding. This was accompanied by decreased expression of UCP1 and mitochondrial respiratory chain functional complexes (mt-Cox1, mt-ND2, and mt-CytB) and mitochondrial genes involved in thermogenic function of brown adipose tissue, such as PRDM16,[35] CPT1, and DIO2. There was also an increase of DGAT-2 in the BAT of *Chem*$^{-/-}$ mice. Therefore, chemerin ablation in mice induced conversion of brown adipocytes to white adipocyte-like cells resulting in decreased BAT activity, a phenomenon seen in patients with obesity or T2D subjects. In agreement with that, *Chem*$^{-/-}$ mice also developed insulin resistance on a high-fat diet or as the *Chem*$^{-/-}$ animals aged, especially in male mice.

As BAT is specialized for energy expenditure and nonshivering thermogenesis, together with whitening of the brown adipocytes seen in *Chem*$^{-/-}$ mice, there was decreased oxygen consumption and CO_2 production, as well as energy expenditure, in the *Chem*$^{-/-}$ mice at ambient temperature (23°C). When energy utilization was examined in *Chem*$^{-/-}$ mice, the respiratory exchange rate of the chem$^{-/-}$ mice was reduced compared to WT mice, reflecting the increased usage of lipid as energy in *Chem*$^{-/-}$ mice.

There are three receptors for chemerin described including CMKLR1 and GPR1, both signaling GPCRs and CCLR2 that does not signal. Chemerin exerts its effect through both

of the GPCRs, CMKLR1, and GPR1. Previous experiments with mice deficient in a single chemerin receptor showed that the GPR1-deficient mouse does not have weight differences when compared to WT fed either a HF or LF diet.[36] In contrast measuring fat content by DEXA, CMKLR1-deficient mice were leaner than WT controls with less fat on both HF and LF diets[37] while another report demonstrated that there is a reduction in weight as well as in lean mass but not fat mass in young CMKLR1-deficient mice compared to WT on normal chow diet.[38] Overall these reports on deficiency in mice of a single chemerin receptor are consistent with our data in which the ligand, chemerin, is ablated.

Our data show that chemerin plays different functional roles in WAT and BAT, although important for differentiation of both WAT and BAT adipocytes. In mature differentiated WAT adipocytes, chemerin is involved in glucose uptake. When chemerin is ablated, a compensatory increase in fatty acid uptake occurs to ensure energy storage is not disrupted due to decreased glucose uptake. Chemerin also modulates the energy balance in brown adipocytes with characteristic small lipid droplets and large mitochondria, maintaining usage of both glucose and fatty acids (Figure 11A). Without chemerin, the energy balance is maintained by using more fatty acids resulting in brown adipocytes with larger lipid droplets and smaller mitochondria resulting in whitening of BAT (Figure 11B). Thus ablation of chemerin alters the energy balance (Figure 11C) with a concomitant increase in the risk of developing insulin resistance, particularly when on a high-fat diet or aging.

Supplementary Material

Refer to Web version on PubMed Central for supplementary material.

ACKNOWLEDGMENTS

These studies were supported by the Maureen Lyles D'Ambrogio Endowed Professorship at the Stanford University School of Medicine and grant (I01BX001959) from the Department of Veterans Affairs (both to LLL) and grant (I01BX000398) from the Department of Veterans Affair and NIH grant P30DK116074 (both to FBK). Figure 11 was partially created with Biorender.com.

Funding information

U.S. Department of Veterans Affairs (VA), Grant/Award Number: I01BX001959; SU | School of Medicine, Stanford University (Stanford University School of Medicine); U.S. Department of Veterans Affairs (VA), Grant/Award Number: I01BX000398; HHS | National Institutes of Health (NIH), Grant/Award Number: P30DK116074

Abbreviations:

Akt	Rac-β serine/threonine protein kinase (protein kinase B)
BAT	brown adipose tissue
CCRL2	chemokine motif receptor-like 2
Chem $^{-/-}$	chemerin-deficient mice
CLAMS	comprehensive laboratory animal monitoring system
CMKLR1	chemokine-like receptor 1

DCs	dendritic cells
DXA	dual energy X-ray absorptiometry
Epi	epdidymal fat
FA	fatty acid
FFA	free fatty acids
GPR-1	G-protein couple receptor 1
HF	high-fat
IL-6	interleukin-6
ipGTT	intra-peritoneal glucose tolerance test
ipITT	intra-peritoneal insulin tolerance test
LF	low-fat
MCP-1	monocyte chemoattractant protein-1
PAI-1	plasminogen activator inhibitor-1
TNF-α	tumor necrosis factor-α
UCP1	uncoupling protein 1
WAT	white adipose tissue
WT	wild-type mice

REFERENCES

1. Giordano A, Smorlesi A, Frontini A, Barbatelli G, Cinti S. White, brown and pink adipocytes: the extraordinary plasticity of the adipose organ. Eur J Endocrinol. 2014;170:R159–R171. [PubMed: 24468979]
2. Cinti S. Transdifferentiation properties of adipocytes in the adipose organ. Am J Physiol Endocrinol Metab. 2009;297:E977–E986. [PubMed: 19458063]
3. Cannon B, Nedergaard J. Brown adipose tissue: function and physiological significance. Physiol Rev. 2004;84:277–359. [PubMed: 14715917]
4. Murano I, Barbatelli G, Giordano A, Cinti S. Noradrenergic parenchymal nerve fiber branching after cold acclimatisation correlates with brown adipocyte density in mouse adipose organ. J Anat. 2009;214:171–178. [PubMed: 19018882]
5. Vitali A, Murano I, Zingaretti MC, Frontini A, Ricquier D, Cinti S. The adipose organ of obesity-prone C57BL/6J mice is composed of mixed white and brown adipocytes. J Lipid Res. 2012;53:619–629. [PubMed: 22271685]
6. Sbarbati A, Morroni M, Zancanaro C, Cinti S. Rat interscapular brown adipose tissue at different ages: a morphometric study. Int J Obes. 1991;15:581–587. [PubMed: 1960009]
7. Cinti S, Frederich RC, Zingaretti MC, De Matteis R, Flier JS, Lowell BB. Immunohistochemical localization of leptin and uncoupling protein in white and brown adipose tissue. Endocrinology. 1997;138:797–804. [PubMed: 9003017]

8. Maury E, Brichard SM. Adipokine dysregulation, adipose tissue inflammation and metabolic syndrome. Mol Cell Endocrinol. 2010;314:1–16. [PubMed: 19682539]
9. Strowig T, Henao-Mejia J, Elinav E, Flavell R. Inflammasomes in health and disease. Nature. 2012;481:278–286. [PubMed: 22258606]
10. Ernst MC, Sinal CJ. Chemerin: at the crossroads of inflammation and obesity. Trends Endocrinol Metab. 2010;21:660–667. [PubMed: 20817486]
11. De Henau O, Degroot GN, Imbault V, et al. Signaling properties of chemerin receptors CMKLR1, GPR1 and CCRL2. PLoS One. 2016;11:e0164179. [PubMed: 27716822]
12. Wittamer V, Franssen JD, Vulcano M, et al. Specific recruitment of antigen-presenting cells by chemerin, a novel processed ligand from human inflammatory fluids. J Exp Med. 2003;198:977–985. [PubMed: 14530373]
13. Monnier J, Lewen S, O'Hara E, et al. Expression, regulation, and function of atypical chemerin receptor CCRL2 on endothelial cells. J Immunol. 2012;189:956–967. [PubMed: 22696441]
14. Goralski KB, McCarthy TC, Hanniman EA, et al. Chemerin, a novel adipokine that regulates adipogenesis and adipocyte metabolism. J Biol Chem. 2007;282:28175–28188. [PubMed: 17635925]
15. Rhee EJ. Chemerin: a Novel Link between Inflammation and Atherosclerosis? Diabetes Metab J. 2011;35:216–218. [PubMed: 21785740]
16. Ge X, Yamaguchi Y, Zhao L, et al. Prochemerin cleavage by factor XIa links coagulation and inflammation. Blood. 2018;131:353–364. [PubMed: 29158361]
17. Zabel BA, Allen SJ, Kulig P, et al. Chemerin activation by serine proteases of the coagulation, fibrinolytic, and inflammatory cascades. J Biol Chem. 2005;280:34661–34666. [PubMed: 16096270]
18. Zhao L, Yamaguchi Y, Ge X, Robinson WH, Morser J, Leung LLK. Chemerin 156F, generated by chymase cleavage of prochemerin, is elevated in joint fluids of arthritis patients. Arthritis Res Ther. 2018;20:132. [PubMed: 29973268]
19. Zhao L, Yamaguchi Y, Sharif S, et al. Chemerin158K protein is the dominant chemerin isoform in synovial and cerebrospinal fluids but not in plasma. J Biol Chem. 2011;286:39520–39527. [PubMed: 21930706]
20. Zhao L, Yamaguchi Y, Shen WJ, Morser J, Leung LLK. Dynamic and tissue-specific proteolytic processing of chemerin in obese mice. PLoS One. 2018;13:e0202780. [PubMed: 30161155]
21. Chang SS, Eisenberg D, Zhao L, et al. Chemerin activation in human obesity. Obesity. 2016;24:1522–1529. [PubMed: 27222113]
22. Ernst MC, Issa M, Goralski KB, Sinal CJ. Chemerin exacerbates glucose intolerance in mouse models of obesity and diabetes. Endocrinology. 2010;151:1998–2007. [PubMed: 20228173]
23. Parlee SD, McNeil JO, Muruganandan S, Sinal CJ, Goralski KB. Elastase and tryptase govern TNFalpha-mediated production of active chemerin by adipocytes. PLoS One. 2012;7:e51072. [PubMed: 23227233]
24. Takahashi M, Takahashi Y, Takahashi K, et al. Chemerin enhances insulin signaling and potentiates insulin-stimulated glucose uptake in 3T3-L1 adipocytes. FEBS Lett. 2008;582:573–578. [PubMed: 18242188]
25. Dubikovskaya E, Chudnovskiy R, Karateev G, Park HM, Stahl A. Measurement of long-chain fatty acid uptake into adipocytes. Methods Enzymol. 2014;538:107–134. [PubMed: 24529436]
26. Barzilai N, Huffman DM, Muzumdar RH, Bartke A. The critical role of metabolic pathways in aging. Diabetes. 2012;61:1315–1322. [PubMed: 22618766]
27. Niccoli T, Partridge L. Ageing as a risk factor for disease. Curr Biol. 2012;22:R741–752. [PubMed: 22975005]
28. Sidossis L, Kajimura S. Brown and beige fat in humans: thermogenic adipocytes that control energy and glucose homeostasis. J Clin Invest. 2015;125:478–486. [PubMed: 25642708]
29. Blaak E. Gender differences in fat metabolism. Curr Opin Clin Nutr Metab Care. 2001;4:499–502. [PubMed: 11706283]
30. Giralt M, Villarroya F. White, brown, beige/brite: different adipose cells for different functions? Endocrinology. 2013;154:2992–3000. [PubMed: 23782940]

31. Muruganandan S, Roman AA, Sinal CJ. Role of chemerin/CMKLR1 signaling in adipogenesis and osteoblastogenesis of bone marrow stem cells. J Bone Miner Res. 2010;25:222–234. [PubMed: 19929432]

32. Roh SG, Song SH, Choi KC, et al. Chemerin–a new adipokine that modulates adipogenesis via its own receptor. Biochem Biophys Res Commun. 2007;362:1013–1018. [PubMed: 17767914]

33. Lorincz H, Katko M, Harangi M, et al. Strong correlations between circulating chemerin levels and lipoprotein subfractions in nondiabetic obese and nonobese subjects. Clin Endocrinol. 2014;81:370–377.

34. Shin HY, Lee DC, Chu SH, et al. Chemerin levels are positively correlated with abdominal visceral fat accumulation. Clin Endocrinol. 2012;77:47–50.

35. Seale P, Kajimura S, Yang W, et al. Transcriptional control of brown fat determination by PRDM16. Cell Metab. 2007;6: 38–54. [PubMed: 17618855]

36. Rourke JL, Muruganandan S, Dranse HJ, McMullen NM, Sinal CJ. Gpr1 is an active chemerin receptor influencing glucose homeostasis in obese mice. J Endocrinol. 2014;222:201–215. [PubMed: 24895415]

37. Ernst MC, Haidl ID, Zuniga LA, et al. Disruption of the chemokine-like receptor-1 (CMKLR1) gene is associated with reduced adiposity and glucose intolerance. Endocrinology. 2012;153: 672–682. [PubMed: 22186410]

38. Issa ME, Muruganandan S, Ernst MC, et al. Chemokine-like receptor 1 regulates skeletal muscle cell myogenesis. Am J Physiol Cell Physiol. 2012;302:C1621–C1631. [PubMed: 22460713]

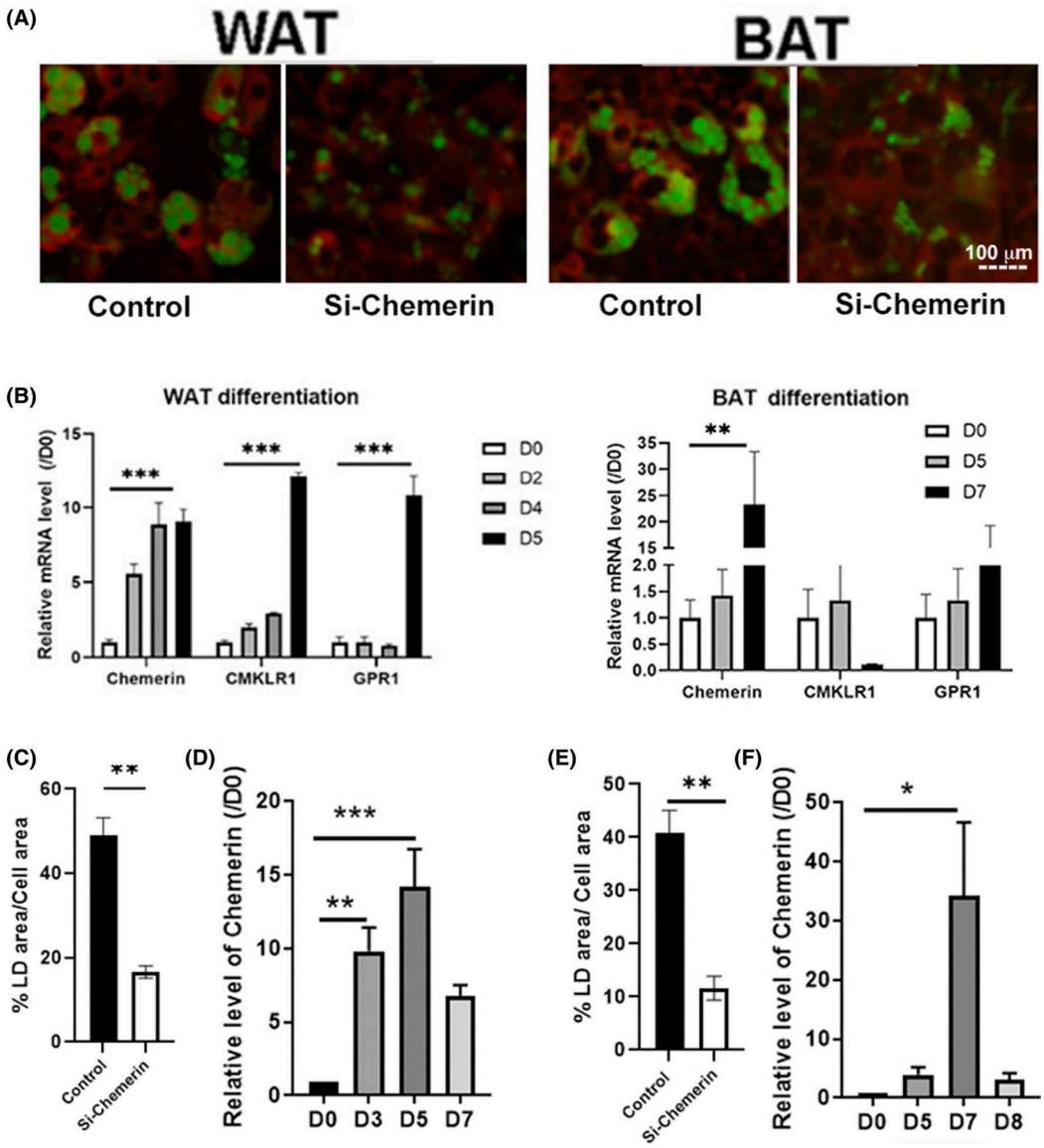

FIGURE 1.

Chemerin is expressed during brown adipocytes differentiation. White (OP9) and brown (SBAT) adipocyte precursor cells were transfected with control and Si-RNA for chemerin before differentiation. A, Staining of cells with mito-tracker (red) and bodipy-FA (green) after 5 days of differentiation for WAT and 7 days after differentiation for BAT. B, Gene expression during adipocyte differentiation. Cells harvested at different days for RNA isolation and analysis of expression of chemerin, CMKLR1, and GPR1. C, Lipid droplet (LD) are shown as ratio to cell area in OP9 cells differentiated with or without chemerin siRNA. D, Relative level of chemerin in culture media of differentiated OP9 adipocytes. E, Lipid droplet (LD) are shown as ratio to cell area in SBAT cells differentiated with or without chemerin siRNA. F, Relative level of chemerin in culture media of differentiated SBAT adipocytes. D0, D3, D5,D7, and D8: days in differentiation medium. Data shown are representative of three independent experiments with n = 3

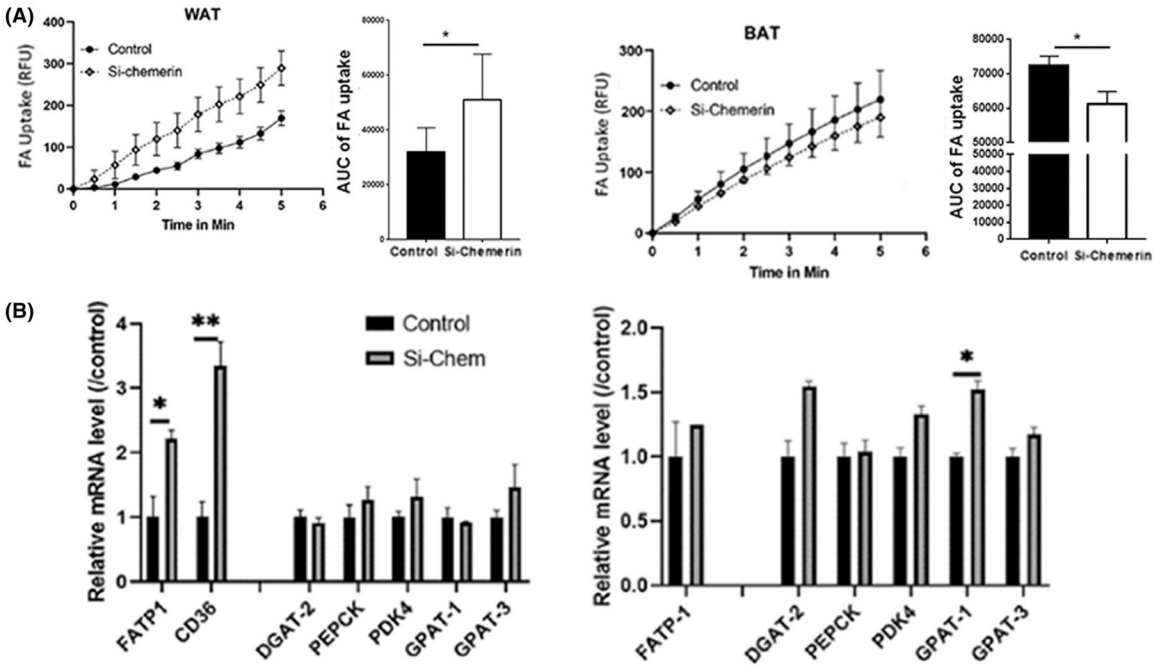

FIGURE 2.

Chemerin is key to brown adipocyte function. A, Effects of knockdown of chemerin in differentiated WAT and BAT cells on FA uptake. B, Relative expression level of genes involved in fatty acid uptake and esterification. These results are representative of 2–3 independent experiments with n = 8 for each assay. **P* < .05, ***P* < .01, ****P* < .001

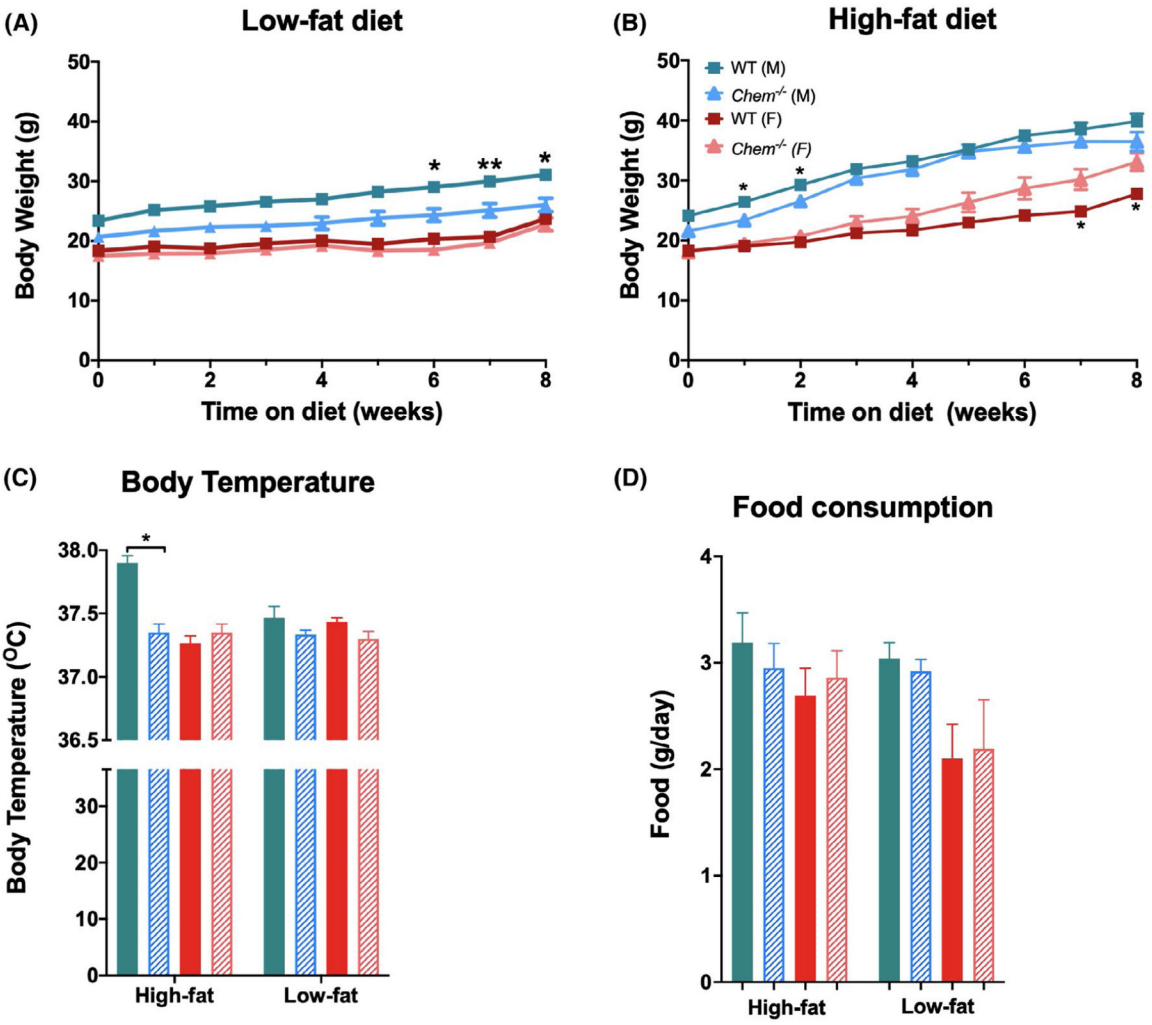

FIGURE 3.

Phenotypic analysis of male and female WT and *Chem*$^{-/-}$ mice on LF and HF diets. A, Growth curve on LF diet. B, Growth curve on HF diet. C, Core body temperature of mice measured at 14 weeks. D, Food consumption/week over 4–7 weeks. Results are presented as mean ± SEM, n = 6–8 for each experiment. **P* < .05, ***P* < .01. WT male (M, ■), *Chem*$^{-/-}$ male (M, ▨), WT female (F, ■) and *Chem*$^{-/-}$ female (F, ▨)

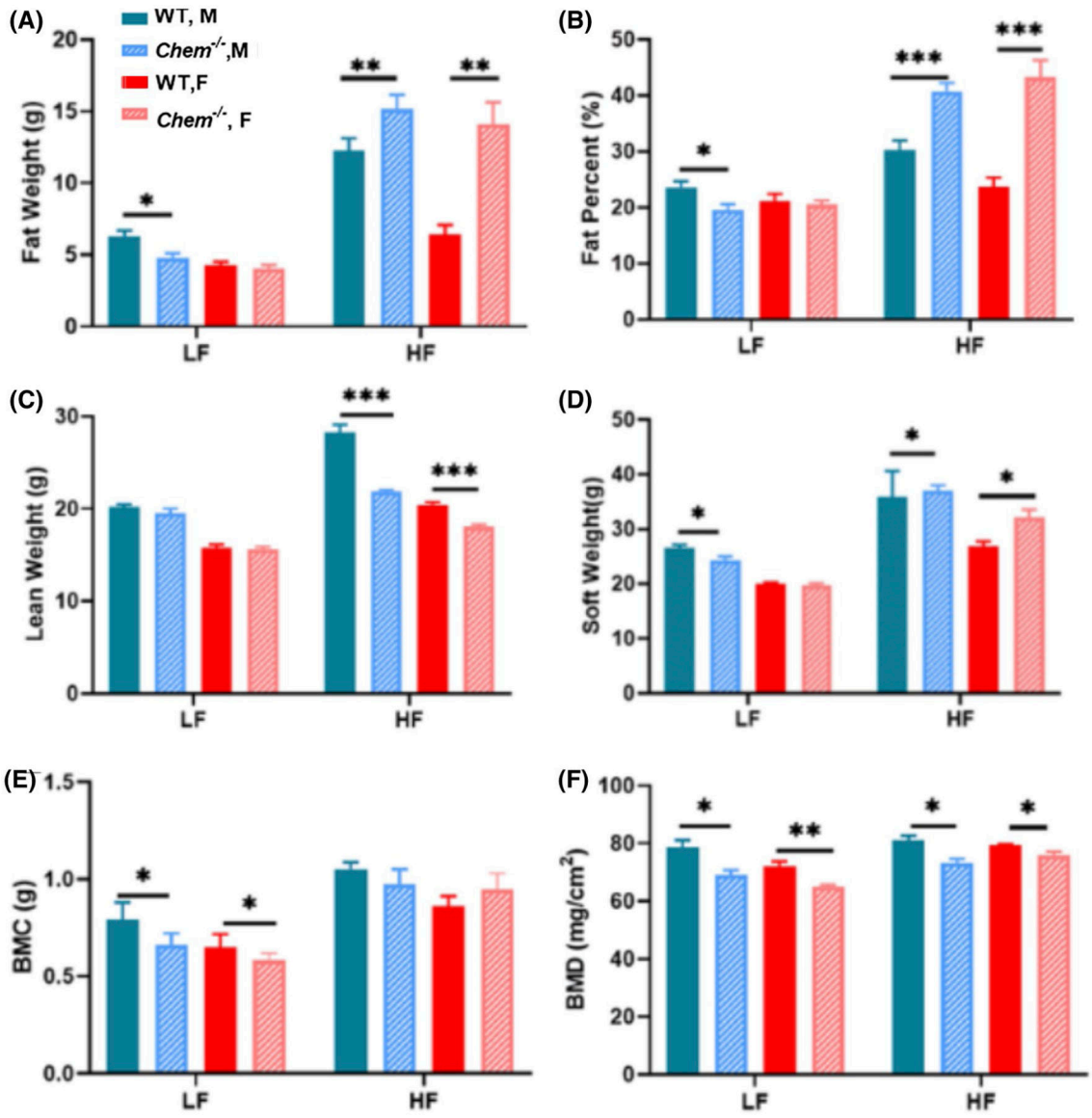

FIGURE 4.

Body composition of male (M) and female (F) WT and *Chem*$^{-/-}$ mice on LF and HF diet. Body composition was determined by DXA after 8 weeks on LF or HF diet. A, Fat weight, (B) Fat percentage, (C) Lean weight, (D) Soft tissue weight, (E) Bone mineral content, (F) Bone marrow density. Results are presented as mean ± SEM with n = 6–8 for each experiment. **P* < .05, ***P* < .01, ****P* < .001

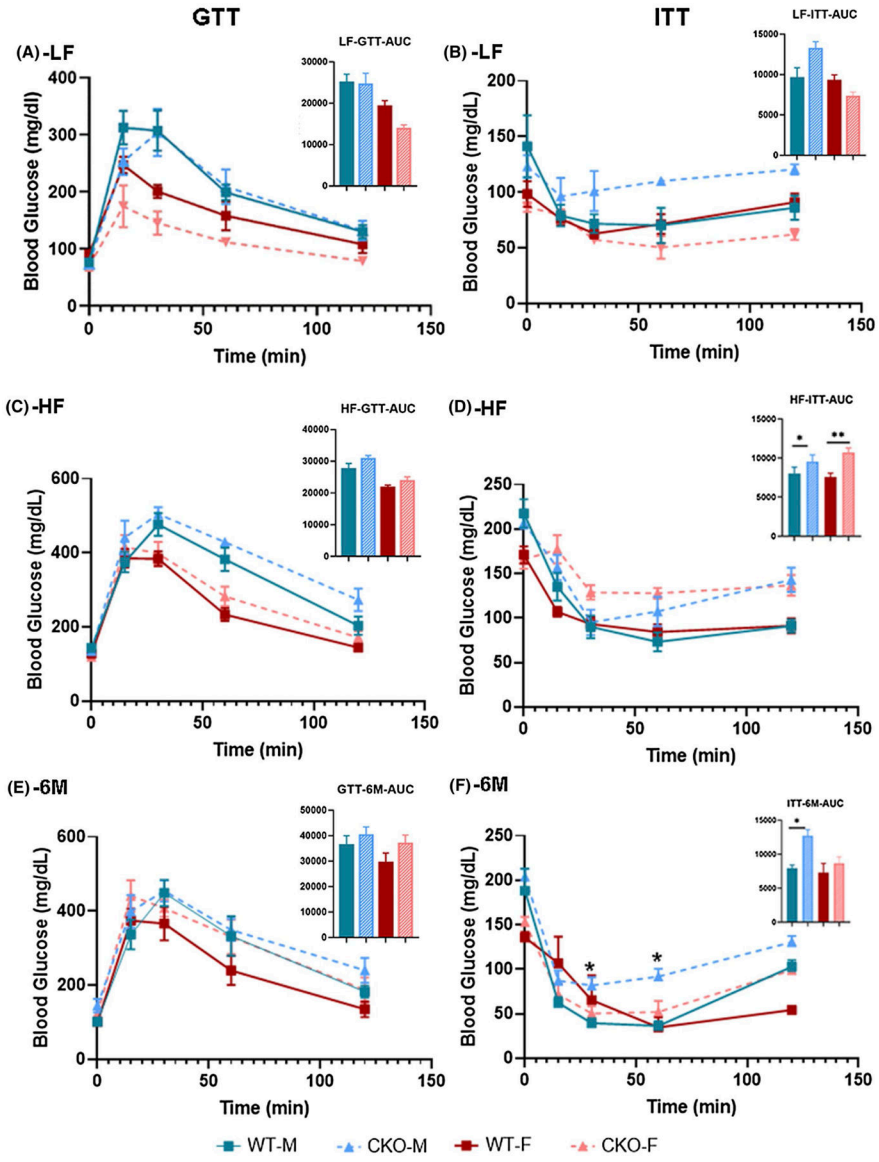

FIGURE 5.

Glucose tolerance test and insulin tolerance test on WT and *Chem*$^{-/-}$ mice on different diets. A, ipGTT of mice on LF diet, (B) ipITT of mice on LF diet, (C) ipGTT of mice on HF diet, (D) ipITT of mice on HF diet, Inset: AUC of ipITT. E, ipGTT of mice at 6 months old, (F) ipITT of mice at 6 months old. Inset: AUC of ipITT. Results are presented as mean ± SEM with n = 6–8 for each experiment. **P* < .05, ***P* < .01

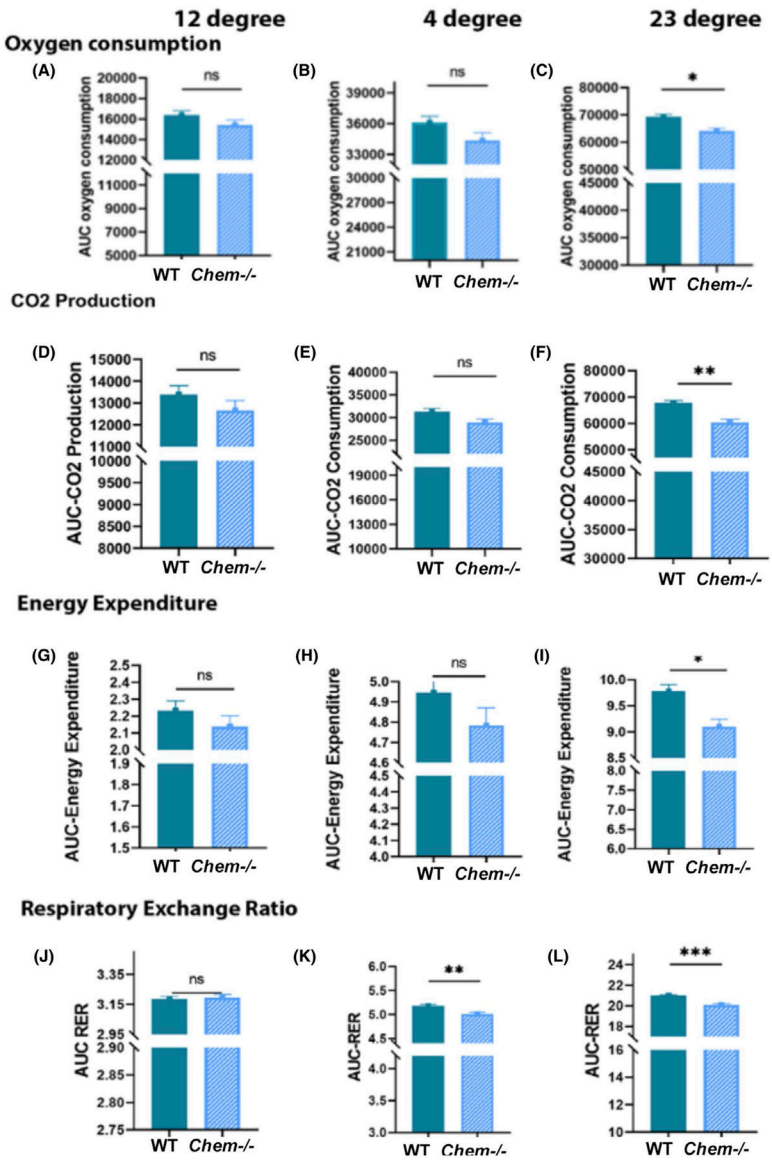

FIGURE 6.

Oxygen consumption, CO2 production, energy expenditure, and respiratory exchange ratio in male WT and *Chem*$^{-/-}$ mice. Results are presented as mean ± SEM with n = 4 for each experiment. **P* < .05, ***P* < .01, ****P* < .001

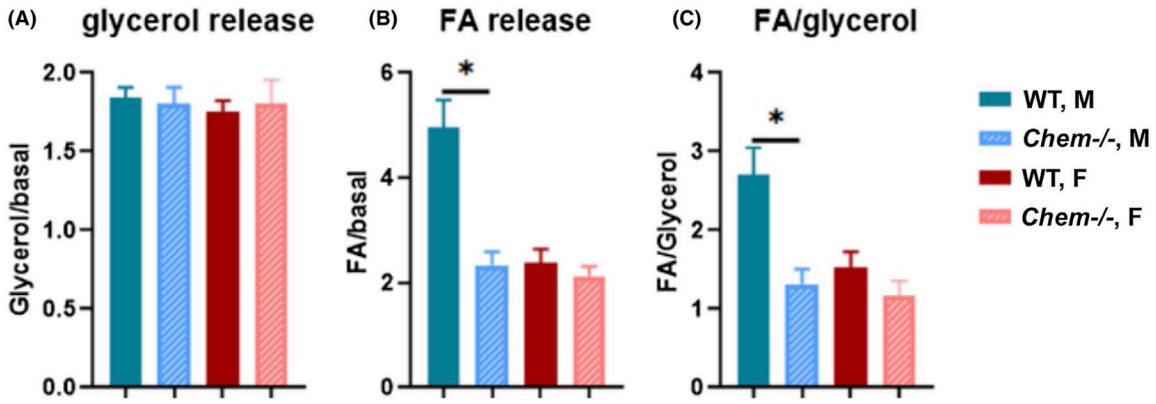

FIGURE 7.

In vivo stimulated lipolysis in male (M) and female (F) WT and *Chem*$^{-/-}$ mice on HF diet. After 8 weeks on HF diet, stimulated lipolysis was determined in mice given ip isoproterenol. A, Glycerol release, (B) FA release, (C) FA/glycerol ratio. Results are presented as mean ± SEM with n = 3–6 for each experiment. *$P < .05$

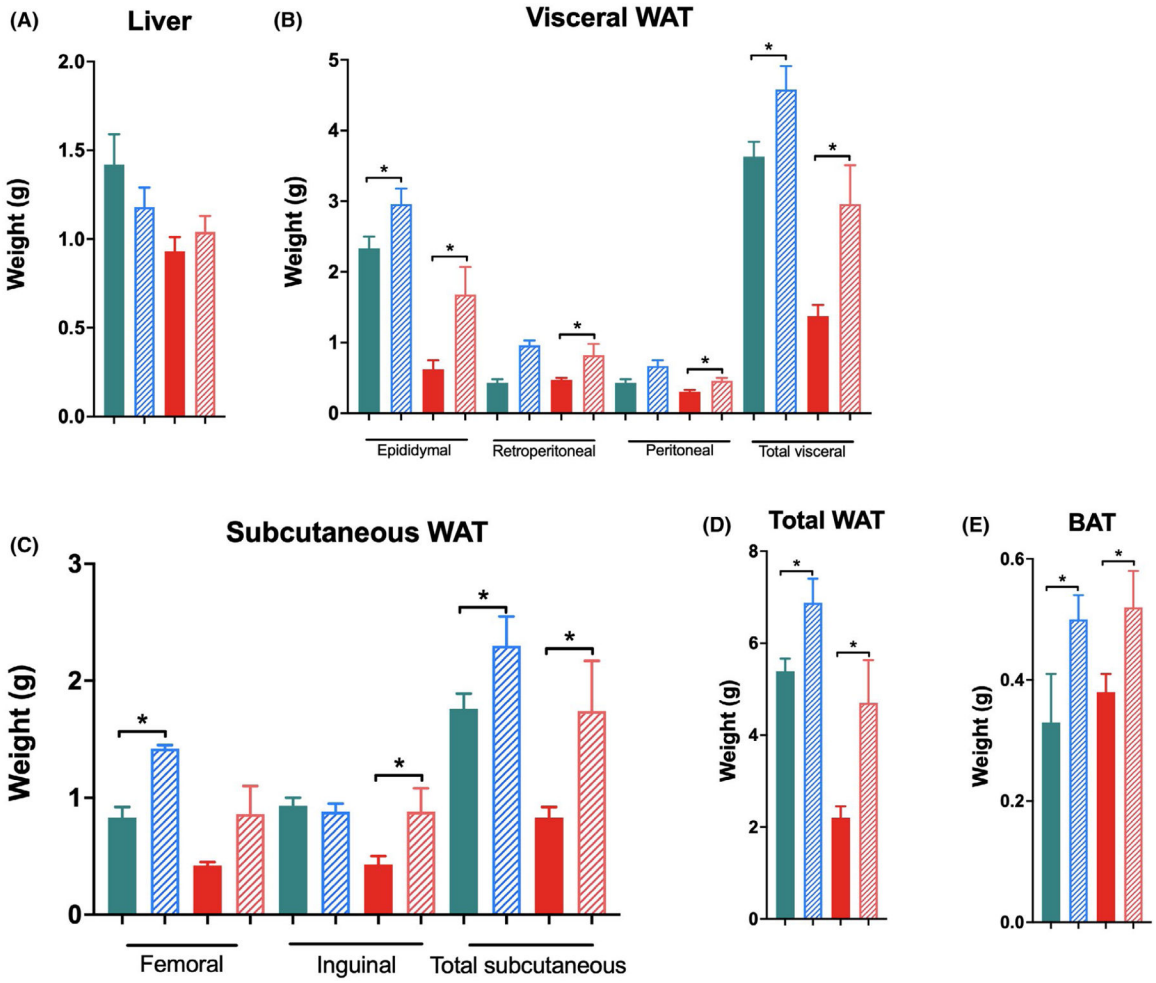

FIGURE 8.

Adipose tissue weights of male and female WT and *Chem*$^{-/-}$ mice on LF and HF diets. A, Liver weight (B) Visceral fat weight (C) Subcutaneous fat weight (D) Total WAT weight (E) BAT weight. Results are presented as mean ± SEM, n = 6–8 for each experiment. **P* < .05, ***P* < .01. WT male (M, ■), *Chem*$^{-/-}$ male (M, ▨), WT female (F, ■) and *Chem*$^{-/-}$ female (F, ▨)

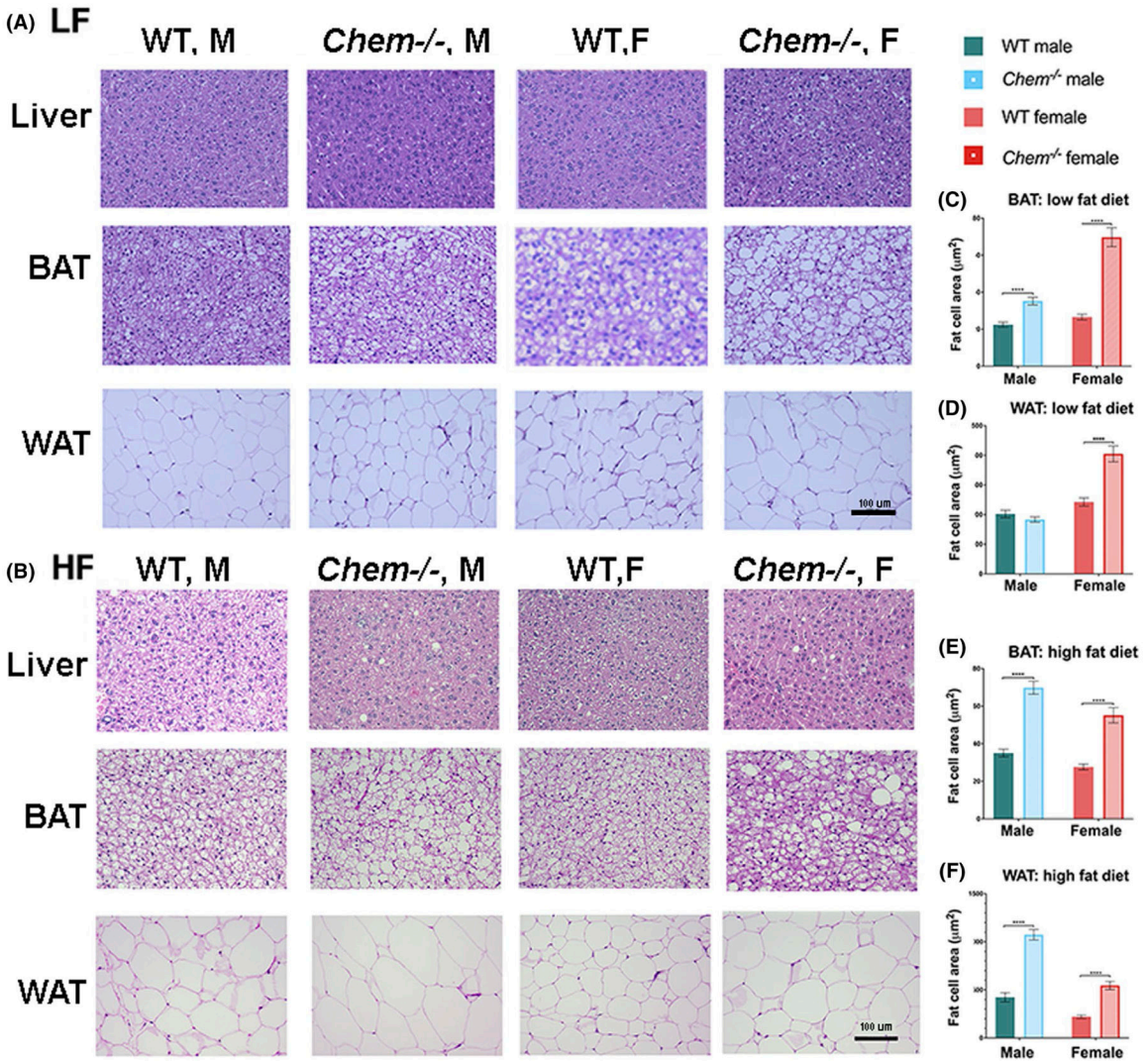

FIGURE 9.

Histological analysis of liver, WAT and BAT from male (M) and female (F) WT and *Chem*$^{-/-}$ mice on LF and HF diet: Liver, WAT, and BAT samples were collected at the time of sacrifice and fixed with 4% paraformaldehyde before paraffin embedding, sectioning, and staining with H&E. Representative images of sections of mice (n = 4 for each group) on LF diet (A), and mice on HF diet (B). Scale bar represent 100 μm. Adipocyte area of 30 random cells was quantitated with ImageJ and shown for BAT on LF diet (C), WAT on LF diet (D), BAT on HF diet (E) and WAT on HF diet (F). **** $P < .0001$

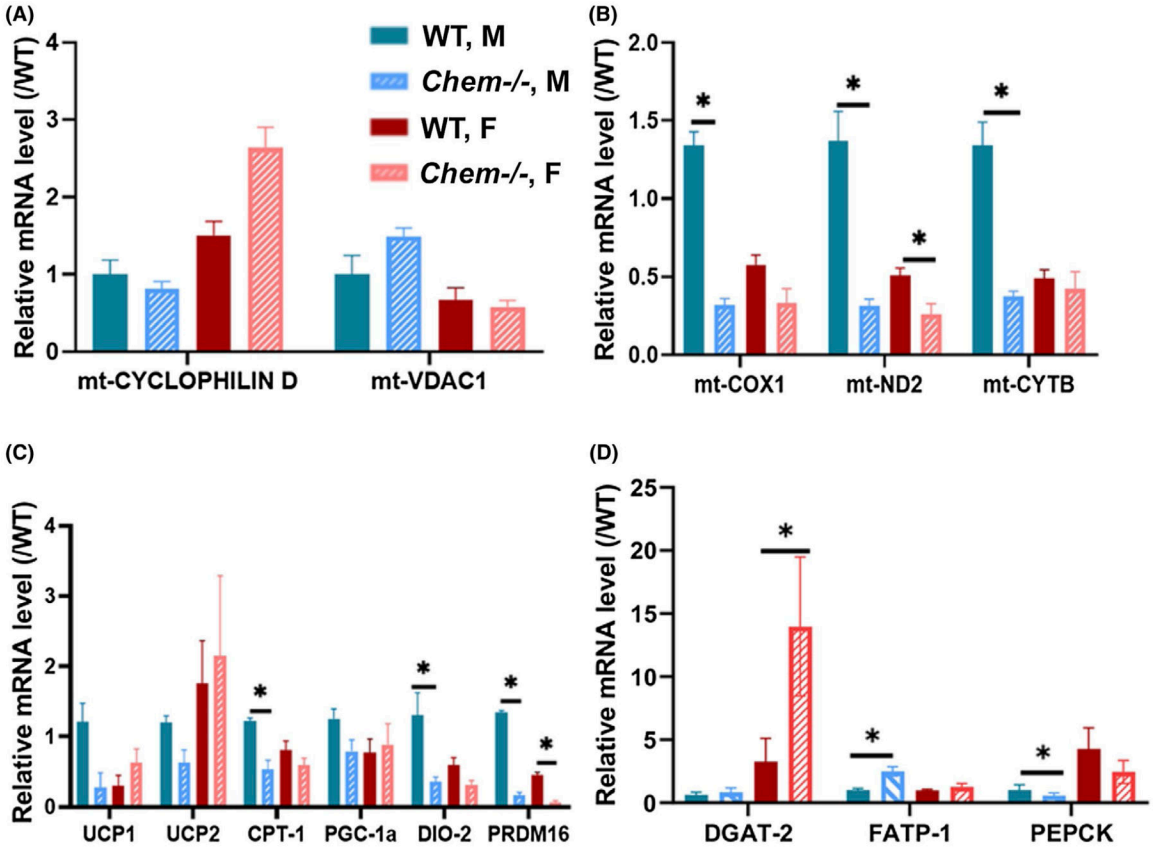

FIGURE 10.

Analysis of gene expression in BAT from male (M) and female (F) WT and *Chem*$^{-/-}$ mice on HF diet. BAT was isolated after 8 weeks on HF diet before being analyzed by rtPCR of mitochondrial genes. A, Mitochondrial gatekeeper genes, (B) Genes involved in mitochondrial respiratory chain function, (C) genes involved in thermogenic function of brown adipose tissue. D, Genes involved in fatty acid uptake and fatty acid esterification. Results are representative of 2–3 independent experiments with n = 3 for each assay. *$P <$ .05

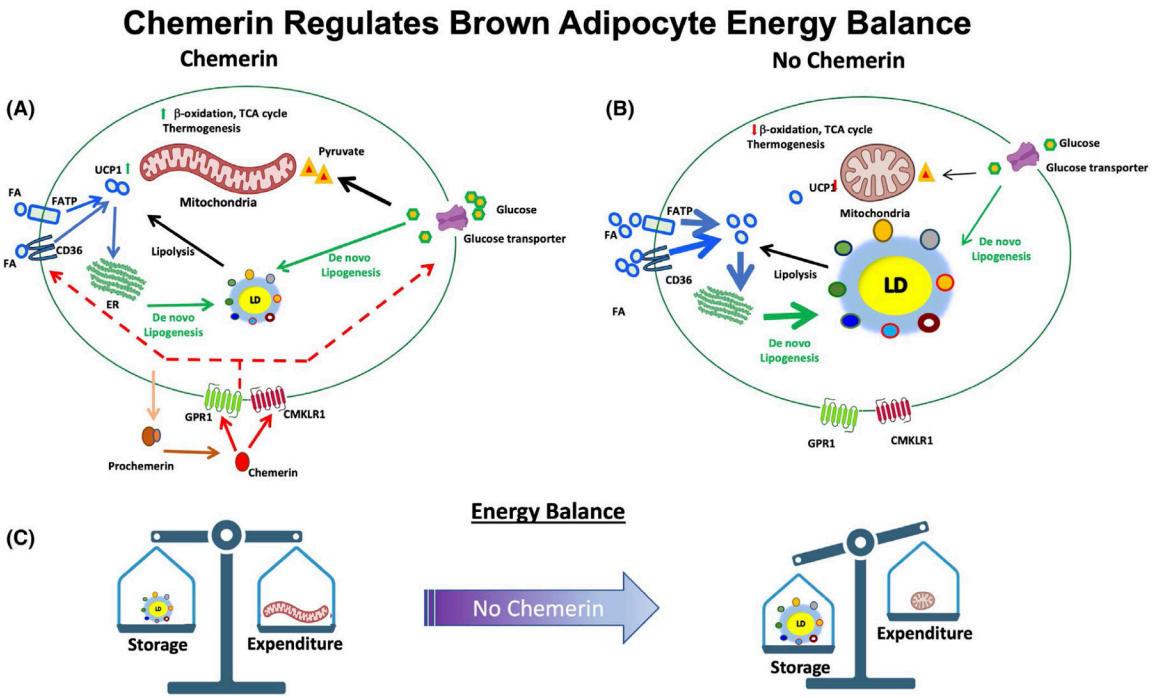

FIGURE 11.

Chemerin regulates brown adipocyte fuel utilization. A, In the presence of chemerin, BAT utilizes both glucose and fatty acids as its fuel sources. Glucose is taken up via the glucose transporter, and then is metabolized to pyruvate, entering the TCA cycle in mitochondria for energy production. Fatty acids can be taken up by CD36 or by fatty acid transporters into the cells. Once inside the cells, fatty acid will be utilized through beta-oxidation and thermogenesis within the mitochondria through increased UCP1 activity. Fatty acids can also go through de novo lipogenesis and stored in the form of TG in lipid droplets. When needed, TG undergoes lipolysis to release fatty acids to enter mitochondria for energy production. Hence there is a balance between glucose and fatty acids in energy utilization. B, Chemerin facilitates glucose uptake, but when ablated, there is decreased glucose uptake into brown adipocytes, hence less pyruvate enters the TCA cycle for energy production. Meanwhile, there is increased fatty acid uptake and esterification resulting in increased lipid droplet deposition in the brown adipocytes and leading to a significant whitening of the BAT. There is no difference in lipolysis, but there is increased re-esterification of fatty acids released from lipolysis and resulting in increased TG storage in lipid droplets. Furthermore, there is decreased UCP1 expression together with decreased mitochondria function and thermogenesis. These changes result in an imbalance between glucose and fatty acid utilization. C, Shows the effect of deletion of chemerin on the energy balance

TABLE 1

Sequence of primers used in the study

Gene	Accession #	Primer sequence
CD36	NM_001159558.1	TGGAGCTGTTATTGGTGCAG TGGGTTTTGCACATCAAAGA
C/EBPβ	NM_001287738	AAGCTGAGCGACGAGTACAAGA GTCAGCTCCAGCACCTTGTG
Chemerin	NM_001347168.1	CTTCTCCCGTTTGGTTTGATT TACAGGTGGCTCCTCTGGAGGAGT
CMKLR1	NM_008153.3	CAAGCAAACAGCCACTACCA TAGATGCCGGAGTCGTTGTAA
CPT-1A	NM_013495	AGACAAGAACCCCAACATCC CAAAGGTGTCAAATGGGAAGG
DGAT2	NM_026384.3	CCGCAAAGGCTTTGTGAAG AGGAATAAGTGGGAACCAGATCAG
DIO2	NM_010050.4	CCATCTCTGCTTCTCGGTCG GCACACATACCACTCAGCACC
FATP1/slc27a1	NM_011977.4	GGCTCCTGGAGCAGGAACA ACGGAAGTCCCAGAAACCAA
GCK	NM_011044.3	GAATCTTCTGTTCCACGGAG AGTGCTCAGGATGTTAAGGA
GPAT1	NM_008149.4	CAACACCATCCCCGACATC GTGACCTTCGATTATGCGATCA
GPAT3	NM_172715.3	GGAGGATGAAGTGACCCAGA CCAGTTTTTGAGGCTGCTGT
GPR1	NM_001357045.1	AAAAGCTGTTTGAGGCTAGAAAGG AGGAAATCTGTTAATGTTCTGTGCG
MT-COX1	MN228594.1	GCTAGCCGCAGGCATTACTA CTCCTCCAGCGGGATCAAAG
MT-Cyclophilin D	NM_001356326.1	CATAGCAGTGCTGACACAGGT TTGGCCAGATACACTCTTGGT
MT-CytB	MN627229.1	CTTCATGTCGGACGAGGCTT CCTCATGGAAGGACGTAGCC
MT-ND2	LC061951.1	ATCCTCCTGGCCATCGTACT ATCAGAAGTGGAATGGGGCG
PDK4	NM_013743.2	GAGGATTACTGACCGCCTCTTTAG TTCCGGGAATTGTCCATCAC
PEPCK	NM_011044.3	ACCCAAGAGCAGAGAGACAC ATGCCCATCCGAGTCATGAT

Gene	Accession #	Primer sequence
PGC-1a	NR_132764.1	GGACAGTCTCCCCGTGGAT TCCATCTGTCAGTGCATCAAATG
PRDM-16	NM_027504.3	CCAGGAGAGCTGCATCAAA CATCACAGGAACACGCTACA
PREF1	NM_001190703	CAGGCAACTTCTGTGAGATCGT TCGTTCTCGCATGGGTTAGG
Rplp0 (36B4)	NM_007475.5	TTTGGGCATCACCACGAAAA GGACACCCTCCAGAAAGCGA
UCP1	AH002110.2	CGATGTCCATGTACACCAAGGA TCGCAGAAAAGAAGCCACAA
UCP2	BC012697.2	GGCCTCTGGAAAGGGACTTC ACCAGCTCAGCACAGTTGACA